Site occupation in the Cr-Ru and Cr-Os σ phases

Marcel H. F. Sluiter*
Department of Materials Science and Engineering, Delft University of Technology, Mekelweg 2, 2628 CD Delft, The Netherlands

Alain Pasturel
Laboratoire de Physique et Modélisation des Milieux Condensés, Maison des Magistères, CNRS, BP 166, 38042 Grenoble Cedex 09, France

(Received 16 June 2009; published 23 October 2009)

The site occupation in the Cr-Ru and Cr-Os σ phases is computed as a function of temperature. Generally, in σ phases the larger atoms occupy the sites with larger coordinations numbers, as can be explained on the basis of atomic-size and electronic structure. However, for Cr_2Ru and Cr_2Os the atomic-size argument predicts that Ru and Os occupy the sites with larger coordination numbers, whereas the reasoning based on the approximate degeneracies of electronic levels predicts that Cr occupies those sites. By comparing these predictions with the theoretically computed and the experimentally measured site occupations, the atomic-size and electronic arguments can be judged on their predictive merits.

DOI: 10.1103/PhysRevB.80.134122 PACS number(s): 61.50.Ks, 61.66.Dk, 71.20.Be, 05.70.Fh

I. INTRODUCTION

The σ phase is a tetrahedrally close-packed phase that occurs in many transition-metal (TM) alloys. In highly alloyed steels and superalloys the occurrence of the σ phase is to be avoided because it is brittle and forms at grain boundaries so that already at low-volume fractions it can strongly degrade the mechanical properties, see, e.g., Refs. 1 and 2, and the corrosion properties, see, e.g., Refs. 3 and 4. The σ phase has a complex tetragonal structure, prototype FeCr, space group $P42/mnm$, with 30 atoms per unit cell that pertain to five crystallographically inequivalent sites with the Wyckoff designations 2a, 4f, $8i_1$, $8i_2$, and 8j.[5–7] As the σ phase is a typical representative of the class of Frank-Kasper (FK) structures,[8,9] sites have characteristic coordination shells with triangular facets only corresponding to 12 (Z12), 14 (Z14), 15 (Z15), and 16 (Z16) nearest neighbors, exclusively. In the σ phase three of those four coordination shells occur: the 2a and $8i_2$ sites are approximately icosahedrally coordinated (Z12), the 4f site has Z15 coordination, and the $8i_1$ and 8j sites have Z14 coordination.

Already long ago Kasper and co-workers[8,9] proposed that among elements of the 3*d* TM series as well as Mo, those to the right of Mn (i.e., Fe, Co, and Ni) prefer Z12 sites in FK structures while those to the left of Mn (i.e., V, Cr, and Mo) prefer Z15 and Z16 sites. The Z14 sites were proposed to have mixed occupancy. Mn anomalously needed to be considered in both groups which was rationalized by referring to the α-Mn structure.[8,9] This scheme was derived from experimental information pertaining to various σ phases but it appeared to be compatible also with data on other FK phases, such as the μ, χ, and Laves phases.[10] Subsequent experimental studies on phases involving 4*d* and 5*d* TMs, summarized in the comprehensive overview by Ansara *et al.*,[11] allowed extension of this description to a wider range of TMs. On the other hand, it was found that generally the site preference of TMs was ruled by the columnar position, i.e., the group number, in the periodic table.[12] Of particular interest is that the average group number, i.e., the valence electron per atom ratio e/a, was found to lie roughly between 6 and 7 for most TM-based FK phases, with σ phases typically occurring between 6.2 and $7.4e/a$. *Ab initio* calculations also indicate this, as was shown previously in Fig. 1 in Ref. 13. It implies that for FK phases between early and late TMs, the composition shifts toward the early TM in the series early TM-Fe, early TM-Co, and early TM-Ni. It should be mentioned that FK phases are by no means restricted to alloys consisting exclusively of TMs as illustrated by the existence of A15 Nb_3Al and Cr_3Si, σ NbAl and TaAl, μMn_6Si, and the Mg-based prototypical Laves phases. In recent years many *ab initio* studies have appeared which all more or less have confirmed the conventional site preference in FK phases.[14–24] Various *ab initio* studies also showed that regardless of the apparent atomic-size differences of the constituent atomic species, relaxation of crystal positions in σ phases is rather small.[15,16] An extensive review of experimentally determined atomic coordinates, also, shows very little dispersion for a wide range of alloys, see Fig. 11 in Ref. 25. It appears that these results argue against atomic size as a determinant for site preference. Hence it appears that there are two conflicting viewpoints for explaining site preference in σ phases and FK phases in general.

Generally, in the theoretical studies it has been difficult to separate size and electronic aspects in the apparent difference between the behavior of early TMs and late TMs because the late TMs typically both are smaller and have larger e/a ratios than early TMs. The atomic-size argument appears more intuitive; a large atom has a larger surface area, allowing for a larger number of nearest neighbors. Thus, larger atoms should occupy the sites with higher occupation numbers. The electronic viewpoint can also be rationalized in a few words: the Z12 sites have approximate icosahedral symmetry causing high degeneracy of electronic *d*-like levels. TM with half-filled *d*-like bands therefore would have very high electronic densities of states if they were to occupy the Z12 sites, which is unfavorable. TM with half-filled *d* bands thus should occupy the higher coordinated sites which allow a better separation of bonding and antibonding *d*-like bands.[13] Generally the atomic-size argument and the electronic argument give the same prediction for the site occupation be-

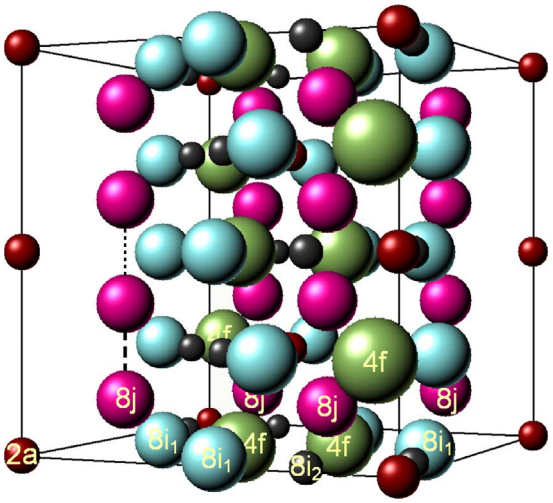

FIG. 1. (Color online) A supercell consisting of two σ unit cells stacked along the c axis, required to determine ECIs associated with two distinct 8j-8j pairs. The two distinct 8j-8j pairs are indicated by a dotted line and a thick dashed line. The inequivalent sites are distinguished by color and size: small red (2a), small black ($8i_2$), large green (4f), large blue ($8i_1$), and large pink (8j).

cause late TM are typically also smaller than early TM. However, a few cases exist where there is discrepancy. Such is the case for the σ phase with approximate composition Cr_2Ru and Cr_2Os where the early TM Cr is smaller in size than the late TMs Ru and Os. Experimental data[25,26] on these systems gives a more or less random site occupation, in contradiction with the earlier stated empirical rules.[11] Here, we will seek to clarify these results theoretically employing *ab initio* density-functional calculations and statistical thermodynamic lattice-gas models.

Currently, two statistical thermodynamic lattice-gas models are in widespread use, the cluster-expansion (CE) method coupled with cluster-variation method (CVM), see Refs. 14–17, 21, and 24, and the so-called compound energy formalism (CEF), see Refs. 19, 20, 22–24, and 27–29. The five inequivalent sites make for $2^5=32$ possible configurations of Cr and Ru(Os) atoms distributed on these sites without breaking any symmetry elements. Typically, within the CEF these configurations only are used. It should be noted that these configurations are not superstructures of the σ phase because they all have the same space group. The CE method, the method used here, requires additional structures because some sites have nearest neighbors (nn) of the same type. Effective cluster interactions (ECIs) for such pairs can be extracted only when pairs formed between sites of the same type have mixed occupancy, necessitating lowering the symmetry of the σ phase. There are actually several compact clusters formed between sites of the same type, in addition to the nn 4f-4f and $8i_2$-$8i_2$ pairs and two distinct $8i_1$-$8i_1$ and 8j-8j pairs, there is a nn triangle formed by three $8i_1$ sites, and a nn tetrahedron between four $8i_1$ sites. Some ECIs, such as those relating to 8j-8j pairs, cannot be determined from configurations involving a single σ unit cell with 30 atoms. The two distinct 8j-8j ECIs require configurations consisting of at least two unit cells (60 atoms) as is illustrated in Fig. 1. Aside from the pairs between equivalent sites, there are also

TABLE I. Number of nearest-neighbor pairs between the various sites within a σ unit cell.

Site	2a	4f	$8i_1$	$8i_2$	8j
2a		4		4	4
4f	4	2	4	8	12
$8i_1$		4	20	16	16
$8i_2$	4	8	16	4	16
8j	4	12	16	16	8

distinct types of pairs between nonequivalent sites. There are three symmetry-unrelated pairs between $8i_1$ and $8i_2$ sites, two symmetry-unrelated 4f-8j pairs, two symmetry-unrelated $8i_1$-8j pairs, and two symmetry-unrelated $8i_2$-8j pairs. To determine interactions associated with these pairs requires at least another five additional structures in which the symmetry of the conventional σ structure is broken. Among nearest-neighbor triangles similar symmetry-unrelated triples exist, e.g., there are four variants of the nearest-neighbor $8i_18i_28j$ triangle, these triples we will ignore in the following. In order to be able to extract all nearest-neighbor effective pair interactions, as well as a number of multibody effective interactions, 13 additional configurations[14–17] were added to the 32 configurations already mentioned.

Usually site preference is discussed on the basis of site-specific properties such as coordination number. However, as is known from atomic ordering on crystal lattices where all positions are equivalent, pairwise terms are very important. Therefore it is of interest to examine also the nearest neighbors of every site. This has been tabulated in Table I.

II. RESULTS AND DISCUSSION

Enthalpies of the 45 configurations have been computed within the local-density approximation using the Vienna *ab initio* simulation program (VASP) (Refs. 30 and 31) at a pressure of 0 GPa. The exchange-correlation functional with generalized-gradient corrections[32] is used. The calculations were performed using pseudopotentials of the projector-augmented wave type.[33,34] The recommended standard potentials[35] were used for Cr, Ru, and Os, which treat the 4s and 3d-, 5s and 4d-, 6s and 5d-like states as valence electrons, respectively. Integrations in reciprocal space use a $4\times4\times8$ Monkhorst-Pack[36] grid in the first Brillouin zone pertaining to the conventional tetragonal unit cell with 30 atoms, giving rise to 12 k points in the irreducible section of the conventional σ structure. In VASP the setting "Precision = Accurate" was employed. In all calculations, the electronic wave functions were expanded in terms of plane waves up to a cutoff kinetic energy of 300 eV. The Hermite-Gauss smearing method of Methfessel and Paxton[37] of order 1 has been used, with a smearing parameter of 0.1 eV, to accelerate k-point convergence. The convergence criteria for energy and force were 0.1 meV and 10 meV/nm, respectively. Structural optimizations were reinitiated at least twice. For final static calculations real-space projectors were turned off and the linear tetrahedron method with Blöchl corrections[38] was used for the reciprocal space integrations.

TABLE II. Computed enthalpies (cohesive energies), lattice parameters, and volume per atom for pure elements (non-spin-polarized).

Elements	Structure	H eV/atom	a (Å)	b (Å)	c (Å)	V (Å^3/atom)
Cr	bcc	−9.468	2.836	2.836	2.836	11.400
Cr	σ	−9.342	8.743	8.743	4.557	11.612
Ru	hcp	−9.162	2.725	2.725	4.304	13.840
Ru	σ	−8.856	9.354	9.354	4.881	14.236
Os	hcp	−11.146	2.757	2.757	4.348	14.315
Os	σ	−10.683	9.462	9.462	4.950	14.775

The enthalpies of formation are computed relative to the stable structures of the pure elements, bcc for Cr, and hcp for Ru and Os,

$$H^{\alpha}_{form} = H^{\alpha} - c^{\alpha}_{\mathrm{Cr}} H_{\mathrm{Cr}} - c^{\alpha}_{X} H_{X}, \quad (1)$$

where X indicates Ru or Os, c represents the atomic concentration, and the enthalpies H are expressed per atom. The properties of the pure-element reference states $H_{\mathrm{Cr}}, H_{\mathrm{Ru}}$, and H_{Os}, listed in Table II, agree well with results published elsewhere.[39,40] The volumes per atom, both for the ground-state crystal structures and for the σ structures clearly indicate that Ru is about 22% larger than Cr and Os is about 26% larger than Cr. The results for the 32σ configurations are listed in Table III and the formation enthalpies [Eq. (1)] are displayed in Fig. 2. As remarked earlier[23] the formation enthalpies for nonmagnetic σ phases have a minimum near the composition A_2B (with A being the early TM and B being the late TM), and this applies to Cr-Ru and Cr-Os as well. Experimentally also, in these systems the σ phase has as approximate composition Cr_2Ru and Cr_2Os. A general explanation can be given using atomic-size arguments: the two sites with the smallest coordination numbers, 2a and $8i_2$, make up one third of the total number of sites, and when these sites are fully occupied by the smaller B-type atoms, a composition A_2B is the result. This explanation is not valid for Cr_2Ru and Cr_2Os because Ru and Os are actually larger than Cr and the site occupancy does not follow atom size as will be discussed later.

It should also be remarked that the σ configurations appear remarkably stable: for all of the 32 Cr-Ru and Cr-Os configurations structural optimizations lead to a structure which can be properly classified as σ on the basis of the characteristic coordination shells mentioned earlier. This was observed previously for almost all pure-element σ configurations.[40,41] However, when the symmetry of the σ structure is broken, e.g., by taking a pure Ru or pure Os σ configuration and placing a Cr atom on only one of the eight 8j sites, structural optimizations can lead to a structure that no longer classifies as a σ configuration because of excessive distortions of the characteristic coordination shells. Therefore, the application of the CE method using low-symmetry structures such as shown in Fig. 1 requires a careful "weeding out" of excessively relaxed structures. This weeding out is not required for the CEF in which all configurations have the full σ symmetry.

TABLE III. Computed formation enthalpies of σ configurations in eV/atom. Configuration is indicated by the occupation of the sites 2a, 4f, $8i_1$, $8i_2$, and 8j, respectively. Energies that are on the convex hull are bold faced.

Configuration	c_{Cr}	$\Delta H(X=\mathrm{Ru})$ eV/atom	$\Delta H(X=\mathrm{Os})$ eV/atom
XXXXX	0.0000	0.3055	0.4629
*XXX*Cr*X*	0.2667	0.1865	0.2587
*XX*Cr*XX*	0.2667	0.2083	0.2922
*XX*Cr*X*Cr*X*	0.5333	0.1540	0.1660
*X*Cr*XXX*	0.1333	0.2696	0.3654
*X*Cr*X*Cr*X*	0.4000	0.1330	0.1573
*X*Cr*X*Cr*XX*	0.4000	0.2282	0.2450
*X*Cr*X*Cr*X*Cr*X*	0.6667	0.1770	0.1545
Cr*XXXX*	0.0667	**0.2650**	**0.3967**
Cr*XX*Cr*X*	0.3333	0.1752	0.2260
Cr*X*Cr*XX*	0.3333	0.1782	0.2282
Cr*X*Cr*X*Cr*X*	0.6000	0.1279	0.1177
CrCr*XXX*	0.2000	0.2263	0.2996
CrCr*X*Cr*X*	0.4667	**0.1066**	0.1140
CrCrCr*XX*	0.4667	0.1949	0.1874
CrCrCrCr*X*	0.7333	0.1521	0.1190
*XXXX*Cr	0.2667	**0.1840**	**0.2146**
*XXX*CrCr	0.5333	0.1110	0.0889
*XX*Cr*X*Cr	0.5333	0.0990	0.0850
*XX*CrCrCr	0.8000	0.1018	0.0805
*X*Cr*XX*Cr	0.4000	0.1711	0.1659
*X*Cr*X*CrCr	0.6667	0.0791	0.0500
*X*Cr*X*Cr*X*Cr	0.6667	0.1186	0.0847
*X*Cr*X*Cr*X*Cr	0.9333	0.1322	0.1233
Cr*XXX*Cr	0.3333	**0.1577**	**0.1687**
Cr*XX*CrCr	0.6000	0.1045	0.0745
Cr*X*Cr*X*Cr	0.6000	0.0851	**0.0525**
Cr*X*CrCrCr	0.8667	0.0988	**0.0682**
CrCr*XX*Cr	0.4667	0.1252	0.1138
CrCr*X*CrCr	0.7333	**0.0632**	**0.0454**
CrCrCr*X*Cr	0.7333	0.1147	0.0735
CrCrCrCrCr	1.0000	0.1265	0.1265

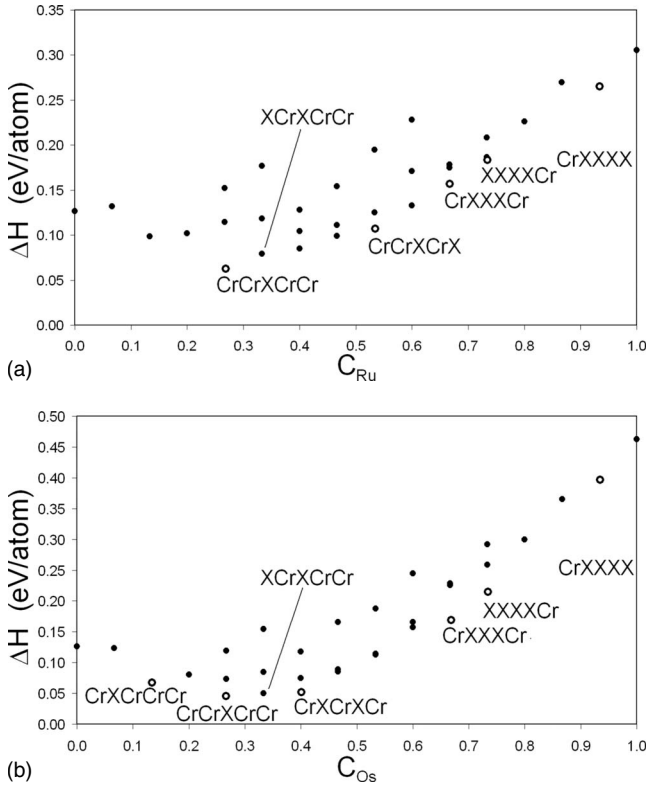

FIG. 2. Formation enthalpies of σ configurations as a function of composition.

The σ configurations on the convex hull, that is the configurations that are ground states when only σ, and not bcc or hcp, are considered are almost the same for Cr-Ru and Cr-Os: for Cr-Ru in order of increasing Cr concentration CrRuRuRuRu, RuRuRuRuCr, CrRuRuRuCr, CrCrRuCrRu, and CrCrRuCrCr; and for Cr-Os in order of increasing Cr concentration CrOsOsOsOs, OsOsOsOsCr, CrOsOsOsCr, CrOsCrOsCr, CrCrOsCrCr, and CrOsCrCrCr. Where it must be noted that the string of five atomic species indicates the occupation of the sites 2a, 4f, $8i_1$, $8i_2$, and 8j, respectively. Considering atomic sizes, one would expect for the composition Cr_2X the configurations Cr*X*?Cr? to be the most stable, where the "?" mark indicates a mixed Cr/*X* occupancy of the $8i_1$ and 8j sites. In Cr_2Ru the calculations point to a mixture of configurations CrCrRuCrRu and CrCrRuCrCr, which contrastingly has a Cr atom at the "large" Z15 coordinated 4f site whereas in Cr_2Os the calculations point to a mixture of configurations CrOsCrOsCr and CrCrOsCrCr, which likewise violates the expectation for the 4f site and which suggests the 4f, $8i_1$, and $8i_2$ as mixed sites rather than the $8i_1$ and 8j sites. It is to be noted that at the composition Cr_2X the configuration *X*Cr*X*CrCr is only just above the convex hull, both for Cr_2Ru and Cr_2Os. The energy of configuration RuCrRuCrCr is close to the average energy of CrCrRuCrRu and CrCrRuCrCr, and the energy of configuration OsCrOsCrCr is close to the average energy of CrOsCrOsCr and CrCrOsCrCr, configurationally the differences are significant. It appears that unlike the previously theoretically studied σ phases,[14–20,22–24] the site occupancy in Cr-Ru and Cr-Os is quite "confused." The structural commonality between RuCrRuCrCr and a mixture of CrCrRuCrRu and CrCrRuCrCr is that the 4f and $8i_2$ sites take Cr and the $8i_1$ site takes Ru whereas the only structural commonality between OsCrOsCrCr and a mixture of CrOsCrOsCr and CrCrOsCrCr is the Cr occupancy of the 8j sites. Surprisingly, our *ab initio* calculations show that Cr-Ru and Cr-Os σ phases are quite different, something that is not apparent from the experimental observations reported by Joubert.[25] Of course, the current analysis is based on configurations where each sublattice is exclusively occupied by a single species. This situation would normally occur at near zero temperature only although not in Cr_2Ru and Cr_2Os which in actuality decompose at low temperature. The effect of temperature on mixed occupation of the sublattices can be expected to be strong because the formation enthalpies for the various σ configurations are very close together, typically about 0.1 eV/atom apart as is apparent in Fig. 2. In Re-W,[15] Re-Ta,[16,17] and Mo-Ru[23] the energy scale is at least twice larger than in the Cr-Ru and Cr-Os systems.

It is evident that Cr and *X* do not have an overwhelming preference for any of the sites. This suggests that, just as in atomic ordering on crystal lattices where all sites are equivalent, pairwise interactions play an important role. Considering that *X* is the minority species, we can try to rationalize the site occupation as follows: starting with a pure Cr σ configuration we substitute all Cr on a sublattice with *X* while counting how many Cr-*X* and *X*-*X* nearest-neighbor pairs are formed, see Table I. If we substitute all Cr by *X* on just one of the eightfold degenerate sites, we notice that the greatest number of Cr-*X* pairs occurs by placing *X* on the 8j sites where it gives 4+12+16+16=48 Cr-*X* pairs (and eight *X*-*X* pairs) and the least number of Cr-*X* pairs occurs by placing *X* on the $8i_1$ site where is gives 4+16+16=36 Cr-*X* pairs (and 20 *X*-*X* pairs). The *ab initio* result listed in Table III indicates that the $8i_1$ site is energetically most preferred and the 8j site is least preferred. This suggests that stable configurations minimize Cr-*X* pairs and maximize *X*-*X* pairs. If, in addition to the $8i_1$ site, either the $8i_2$ or the 8j site is substituted with *X*, the nn pair analysis suggests that both are about equally preferred. This is indeed the case, the CrCr*XX*Cr and CrCr*X*Cr*X* energies are close and are well below the CrCrCr*XX* energy. The maximal number of *X*-*X* pairs for Cr_2X is achieved when Cr fully occupies the 2a and 4f sites, *X* fully occupies the $8i_1$ site, and the $8i_2$ takes 10% *X* and the 8j site takes 15% *X*. The nn pairwise analysis seems more capable of explaining site preferences than arguments based on the characteristics of a specific sublattice such as atomic-size/coordination number or approximate point symmetry. A tantalizing feature is that maximizing *X*-*X* pairs and minimizing unlike (Cr-*X*) pairs is symptomatic of a phase separating system, although the Cr-Ru and Cr-Os systems are compound forming. The known Cr-*X* compounds are the σ Cr_2X phases studied here, and the tetrahedrally close-packed A15 Cr_3X phases. Clearly, these compounds are not conventional superstructures of bcc, fcc, or hcp and therefore one may not deduct simply that the effective pair interactions favor unlike pairs. The considerable atomic volume differences between Cr and Ru (23%) and Cr and Os (27%) make miscibility gaps on both the bcc and hcp lattices quite likely at lower temperatures.

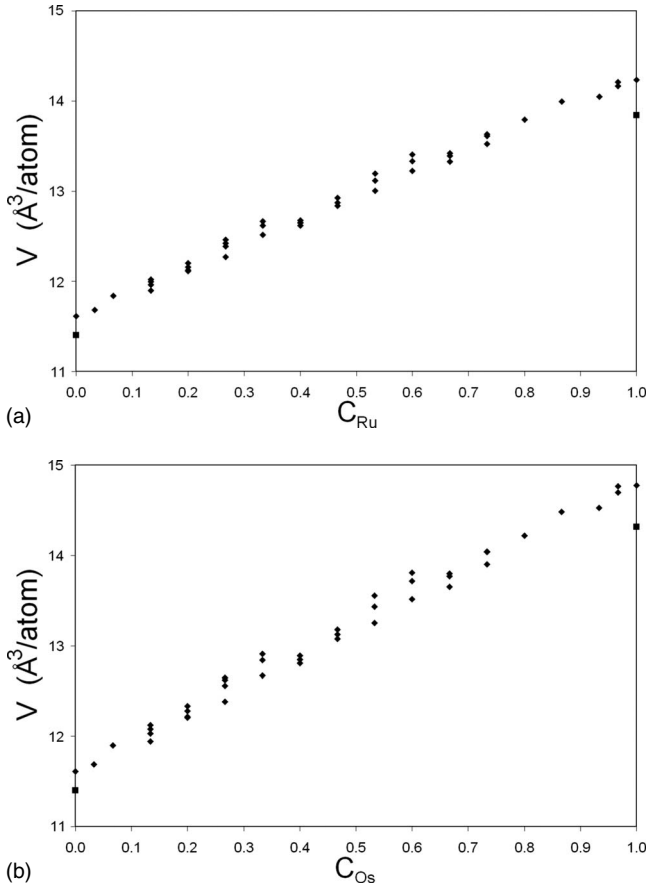

FIG. 3. Equilibrium volume as a function of composition; squares pertain to elemental reference states, diamonds to σ configurations.

In alloys where intermixing produces small excess enthalpies, volumes per atom often follow an approximately linear variation with composition, such is apparent in Fig. 3. Where there is strong bonding, interatomic distances and volumes often contract relative to the linear variation but in Cr-Ru and Cr-Os there is no significant correlation between volume contraction and formation enthalpy. It can be noted however, that the pure-element ground states are more compact than the not stable pure-element σ configurations. The Cr σ phase has a 2% larger volume than the stable bcc phase, and for Ru and Os the σ phase is 3% less compact than the stable hcp phase.

The value of the internal coordinates of the 32 structures with the symmetry of the σ structure is shown in Fig. 4. The variation is somewhat larger than that found by Joubert (see Fig. 11 in Ref. 25) in the experimental measurements but the spread is still rather small considering the large volume differences between Cr and Ru, Os (see Table II). It should be remarked that the experiments naturally consider stable, or metastable, and often somewhat disordered configurations. The theoretically computed internal coordinates include highly unstable configurations also, as well as σ configurations that are far removed from their usual composition so that a slightly larger spread is to be expected. Figure 4 shows that the five internal coordinates cannot relax much, regardless of the atomic-size difference between the constituent atoms, as we have earlier seen in Re-W and Ta-W σ phases.[15–17] Apparently the coordination shells Z12, Z14, and Z15 are very stiff.

Above it was shown that in Cr-Ru and Cr-Os it is not readily apparent that one can evaluate directly the site occupation by inspecting zero-temperature enthalpies of configurations with sublattices filled exclusively by a single atomic species. Experimental evidence[25] points to mixed occupancy on all of the sublattices at finite temperature. Therefore, here the effect of temperature on the site occupation will be examined in detail with the CE-CVM. I select the CE-CVM method instead of the CEF method because the former allows incorporation of the effects of the various symmetry-distinct pairs and triangles discussed above.

Figure 5 shows that the site occupation in $Cr_{0.668}Ru_{0.332}$ is rather intermixed at temperatures of interest. The horizontal lines indicate the site occupation as an average of three experimental measurements,[25,26,42] see Table IV in Ref. 25. The experimental determinations are all rather close, largest variations in the site occupations of about $12a/o$ occurring for sites $8i_2$ and 8j. The experimental measurements were carried out on samples annealed at 1573 (Ref. 26) and 1673 K.[25] Experimentally, Ru prefers three sites about equally: $8i_1$, 4f, and $8i_2$ while Ru avoids the 2a and 8j sites. A rather similar sequence is seen in our *ab initio* CE-CVM computations. It is of interest to compare with the predictions based on simple models, see Table IV. It is apparent that none of the three models, atomic-size/coordination number (size), least unlike pairs (pairs), electronic degeneracy (degeneracy), correctly captures that $8i_1$, 4f, and $8i_2$ have about equal affinity toward Ru, and that 2a and 8j have about equal affinity for Cr. "Size" mixes up the behavior of $8i_2$ and 8j, "pairs" mixes up 4f and 8j, and "degeneracy" fails on the 2a, 4f, and $8i_1$ sites. Looking site by site, 4f is characterized properly only by size, $8i_1$ and 2a are characterized correctly according to size and pairs, $8i_2$ requires pairs and degeneracy while 8j is described by degeneracy only. It is evident that a correct characterization of every site requires both size and degeneracy arguments in the least, possibly augmented by pairs. The combination of all three arguments could be invoked to explain the site occupation in an admittedly debatable manner; Ru prefers $8i_1$ because of minimizing Cr-Ru pairs and because of atomic size; 4f is weakly preferred because of atomic size in spite of electronic degeneracy and in spite of unfavorable Cr-Ru pairs; the $8i_2$ site is not avoided by Ru because of favorable electronic degeneracy in spite of atomic size.

The agreement between experiment and CE-CVM can be evaluated through a root of the mean squares (rms) of the differences with the experimental site occupations, this is plotted in Fig. 6. Although the experimental site occupations apply to a temperature of about 1600 K, and the computed values are temperature-dependent equilibrium values, it is clear that much higher temperatures the CE-CVM agrees best with experiment. This reflects the fact that experimentally the site occupation is more intermixed than in the computations. Particularly, the $8i_1$, 4f, 8j, and 2a sites deviate more from the average fraction Ru of 0.332 than in experiment.

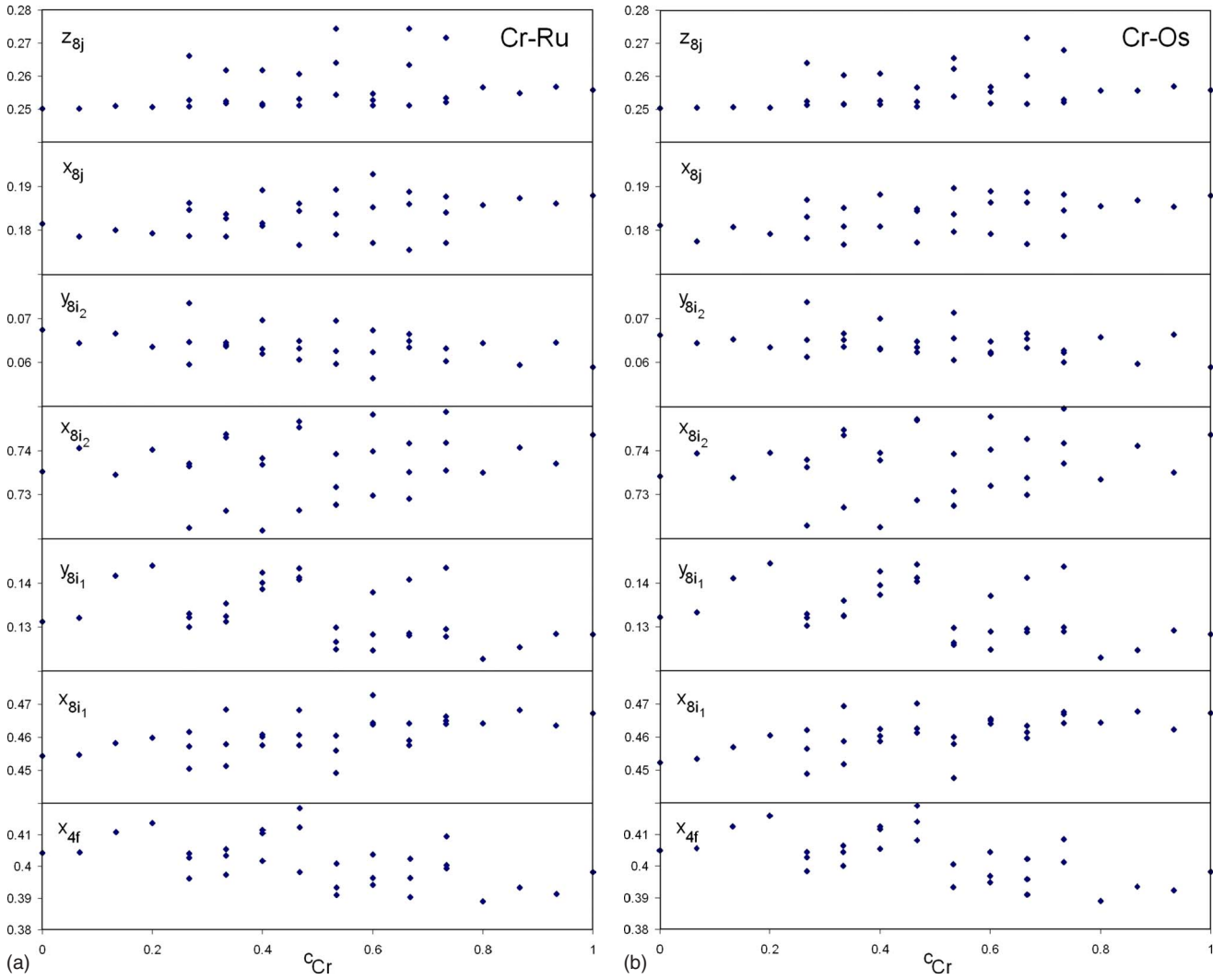

FIG. 4. (Color online) Internal coordinates of σ configurations.

In Cr-Os the site occupations are intermixed also, just a little less than in the Cr-Ru system, as is readily apparent from comparing Fig. 7 with Fig. 5. In Fig. 7 the horizontal lines indicate the site occupation as an average of two experimental measurements,[25,26] see Table IV in Ref. 25. The experimental determinations are close, all sites agreeing within a few percent with the exception of the $8i_2$ site where Alte da Veiga *et al.*[26] give an occupation that is $9a/o$ higher in Os than Joubert.[25] The experimental measurements were carried out on samples annealed at 1673 (Ref. 26) and 1873 K.[25] Experimentally, Os prefers the five sites in a similar sequence as Ru, see also Table IV. As in Cr_2Ru, the sites can be separated in two groups, the high-Cr sites: 8j and 2a; and the low-Cr sites: 4f, $8i_1$, and $8i_2$. The CE-CVM calculations correctly reproduce the grouping. The characterization of site occupation according to size, pairs, and degeneracy follows the same lines as for Cr-Ru discussed above with none of the arguments alone capable of explaining observed and *ab initio* computed site occupations. A combination of arguments might be invoked to try to explain the site occupation;

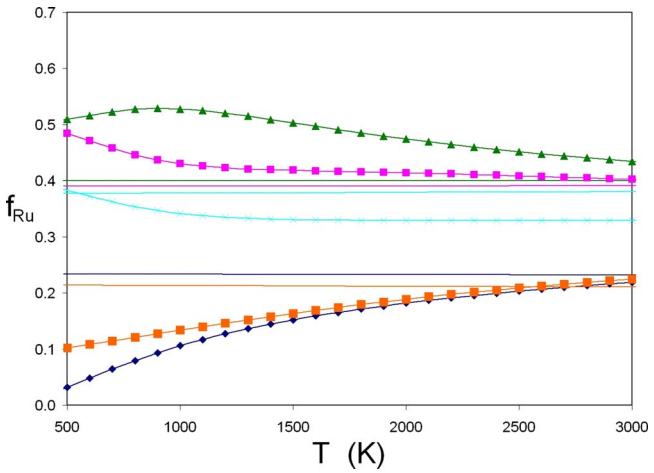

FIG. 5. (Color online) Site occupation in $Cr_{0.668}Ru_{0.332}$ as function of temperature as computed with CE-CVM; green triangles: $8i_1$, pink squares: 4f, blue crosses: $8i_2$, orange squares: 8j, and black diamonds: 2a. Horizontal lines indicate averaged experimentally determined values at approximately 1600 K (Ref. 25).

TABLE IV. Site occupation according to various considerations and methods in Cr_2Ru and Cr_2Os.

Method	Increasing Cr affinity→				
Atomic size	4f	$(8i_1,8j)$			$(8i_2,2a)$
Least unlike pairs	$8i_1$	$(8j,8i_2)$			(4f,2a)
e^- degeneracy	$(8i_2,2\ a)$				$(4f,8i_1,8j)$
$Cr_{0.667}Ru_{0.333}$: expt.[a]	$8i_1$	4f	$8i_2$		(2a,8j)
$Cr_{0.658}Ru_{0.342}$: expt.[b]	$8i_2$	$8i_1$	4f	2a	8j
$Cr_{0.668}Ru_{0.332}$: expt.[c]	4f	$8i_1$	$8i_2$		(2a,8j)
$Cr_{0.668}Ru_{0.332}$: CE-CVM	$(8i_1,4f,8i_2)$				(8j,2a)
$Cr_{0.67}Os_{0.33}$: expt.[b]	$8i_2$	4f	$8i_1$	2a	8j
$Cr_{0.693}Os_{0.307}$: expt.[c]	4f	$(8i_1,8i_2)$			(8j,2a)
$Cr_{0.68}Os_{0.32}$: CE-CVM	$(8i_2,8i_1,4f)$				(8j,2a)

[a]Reference 42.
[b]Reference 26.
[c]Reference 25.

Os prefers 4f because of its size, it also has affinity to $8i_2$ in spite of its low coordination number because of low numbers of Cr-Os pairs and because of favorable electronic degeneracy; $8i_1$ also is weakly preferred because of all three arguments; and the remaining 2a and 8j sites are Cr occupied by default. The rms of the differences between CE-CVM and experimental site occupations exhibits a minimum just above 2500 K, see Fig. 6. This appears roughly in the vicinity of the experimental annealing temperature but more probable is that it is a fortuitous agreement given the rather large differences in site occupation between experiment and CE-CVM.

III. CONCLUSION

The site occupation in Cr_2Ru and Cr_2Os as computed here shows a rather intermixed behavior just as has been found experimentally.[25,26,42] There is no strong correlation with either coordination number or approximate point symmetry. This means that neither atomic-size nor electronic-degeneracy arguments can explain the actual site occupations. Site occupation is equally well, or equally poorly, explained by minimization of nearest-neighbor unlike bonds. A combination of arguments based on atomic size, electronic degeneracy, and least unlike pairs could be made to explain site occupations but this has no predictive value because of arbitrariness. Unlike pairs being unfavorable points toward phase-segregating tendencies in Cr_2Ru and Cr_2Os alloys. Curiously, in the A15 Cr_3Si prototype phases with compositions Cr_3Ru (Ref. 43) and Cr_3Os,[44] a strong correlation between site occupation and coordination number or approximate point symmetry is assumed[45] on the basis of the composition. In these compounds Cr is believed[45] to occupy the more highly coordinated Z14 sites while Ru and Os are believed to occupy the approximate icosahedral Z12. While these site occupations would agree perfectly with that predicted by electronic-degeneracy arguments, it might be worthwhile to

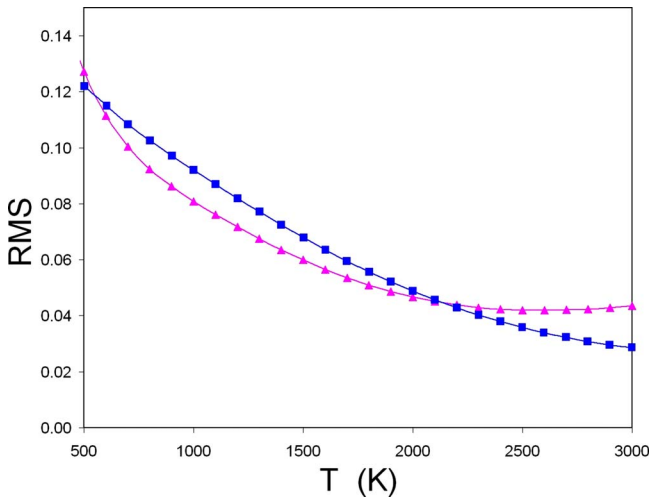

FIG. 6. (Color online) rms of difference between computed and experimentally measured site occupation as function of temperature in $Cr_{0.668}Ru_{0.332}$ (blue squares) and $Cr_{0.68}Os_{0.32}$ (pink triangles).

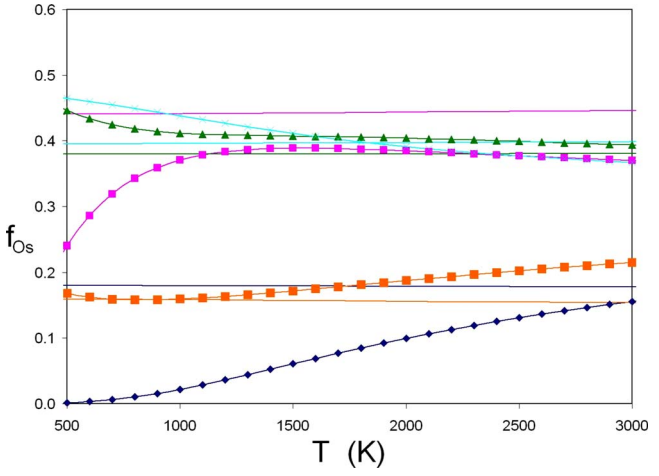

FIG. 7. (Color online) Site occupation in $Cr_{0.68}Os_{0.32}$ as function of temperature as computed with CE-CVM; green triangles: $8i_1$, pink squares: 4f, blue crosses: $8i_2$, orange squares: 8j, and black diamonds: 2a. Horizontal lines indicate averaged experimentally determined values at approximately 1800 K (Ref. 25).

actually verify it because the σ phase behaves so differently.

The CE-CVM approach for treating the σ phase was shown to require many additional structures in order to extract effective interactions associated with nonequivalent clusters. The additional structural energies generally pertain to structures where sublattices have mixed occupancy, that is, where the symmetry of the original structure is broken. Such symmetry lowering may result in structural relaxations and deformations, and one must carefully verify that relaxation is not so excessive as to disturb coordination shells and other local structural features.

ACKNOWLEDGMENTS

M.S. acknowledges support by "Materials Innovation Institute" (www.m2i.nl) in collaboration with the Foundation for Fundamental Research on Matter (FOM) of the Netherlands under Project No. 02EMM032. The National Computer Facilities of the Netherlands Foundation for Scientific Research (NWO) are gratefully acknowledged for computer resources provided under Grant No. SH-007-07. A.P. gratefully acknowledges "College van Bestuur" and the hospitality of the University of Technology Delft.

*m.h.f.sluiter@tudelft.nl

[1] H. Sieurin and R. Sandström, Mater. Sci. Eng., A **444**, 271 (2007).
[2] D. M. E. Villanueva, F. C. P. Junior, R. L. Plaut, and A. F. Padilha, Mater. Sci. Technol. **22**, 1098 (2006).
[3] M. E. Wilms, V. J. Gadgil, J. M. Krougman, and F. P. Ijsseling, Corros. Sci. **36**, 871 (1994).
[4] N. Lopez, M. Cid, and M. Puiggali, Corros. Sci. **41**, 1615 (1999).
[5] E. Hall and S. Algie, Metall. Rev. **11**, 61 (1966).
[6] J. L. C. Daams, P. Villars, and J. H. N. van Vucht, *Atlas of Crystal Structures for Intermetallic Phases* (ASM International, Materials Park, OH, 1991), p. 3804.
[7] C. B. Shoemaker and D. P. Shoemaker, in *Developments in the Structural Chemistry of Alloy Phases*, edited by B. C. Giessen (Plenum, New York, 1969), p. 107.
[8] J. S. Kasper, *Atomic and Magnetic Ordering in Transition Metal Structure in Theory of Alloy Phases* (ASM, Cleveland, OH, 1956), p. 264.
[9] J. S. Kasper and R. M. Waterstrat, Acta Crystallogr. **9**, 289 (1956).
[10] J. S. Kasper, Acta Metall. **2**, 456 (1954).
[11] I. Ansara, B. Burton, Q. Chen, M. Hillert, A. Fernandez-Guillermet, S. G. Fries, H. L. Lukas, H.-J. Seifert, and W. A. Oates, CALPHAD: Comput. Coupling Phase Diagrams Thermochem. **24**, 19 (2000).
[12] M. V. Nevitt, in *Electronic Structure and Alloy Chemistry of Transition Elements*, edited by P. A. Beck (Interscience, New York, 1963), p. 101.
[13] C. Berne, A. Pasturel, M. Sluiter, and B. Vinet, Phys. Rev. Lett. **83**, 1621 (1999).
[14] M. H. F. Sluiter, K. Esfarjani, and Y. Kawazoe, Phys. Rev. Lett. **75**, 3142 (1995).
[15] C. Berne, M. H. F. Sluiter, Y. Kawazoe, T. Hansen, and A. Pasturel, Phys. Rev. B **64**, 144103 (2001).
[16] C. Berne, M. H. F. Sluiter, Y. Kawazoe, and A. Pasturel, J. Phys.: Condens. Matter **13**, 9433 (2001).
[17] C. Berne, M. H. F. Sluiter, and A. Pasturel, J. Alloys Compd. **334**, 27 (2002).
[18] J. Havrankova, J. Vrestal, L. G. Wang, and M. Sob, Phys. Rev. B **63**, 174104 (2001).
[19] J. Houserova, M. Friak, M. Sob, and J. Vrestal, Comput. Mater. Sci. **25**, 562 (2002).
[20] J. Houserova, J. Vrestal, M. Friak, and M. Sob, CALPHAD: Comput. Coupling Phase Diagrams Thermochem. **26**, 513 (2002).
[21] M. H. F. Sluiter, A. Pasturel, and Y. Kawazoe, Phys. Rev. B **67**, 174203 (2003).
[22] P. Korzhavyi, B. Sundman, M. Selleby, and B. Johansson, in *Integrative and Interdisciplinary Aspects of Intermetallics*, MRS Symposia Proceedings Vol. 842 (Materials Research Society, Pittsburgh, 2005), p. S4.10.1.
[23] O. Grånäs, P. A. Korzhavyi, A. E. Kissavos, and I. A. Abrikosov, CALPHAD: Comput. Coupling Phase Diagrams Thermochem. **32**, 171 (2008).
[24] M. Sluiter, A. Pasturel, and Y. Kawazoe, *Prediction of Site Preference and Phase Stability of Transition Metal Based Frank-Kasper Phases in The Science of Complex Alloy Phases*, edited by P. E. A. Turchi and T. Massalski (TMS, Warrendale, PA, USA, 2005) p. 409.
[25] J.-M. Joubert, Prog. Mater. Sci. **53**, 528 (2008).
[26] L. M. Alte da Veiga, M. M. R. R. Costa, M. J. M. de Almeida, L. R. Andrade, and A. Matos Beja, Acta Crystallogr., Sect. B: Struct. Crystallogr. Cryst. Chem. **36**, 1750 (1980).
[27] S. G. Fries and B. Sundman, Phys. Rev. B **66**, 012203 (2002).
[28] N. Dupin, S. G. Fries, J.-M. Joubert, B. Sundman, M. Sluiter, Y. Kawazoe, and A. Pasturel, Philos. Mag. **86**, 1631 (2006).
[29] J. Vrestal, A. Kroupa, and M. Sob, Comput. Mater. Sci. **38**, 298 (2006).
[30] G. Kresse and J. Furthmüller, Comput. Mater. Sci. **6**, 15 (1996).
[31] G. Kresse and J. Furthmüller, Phys. Rev. B **54**, 11169 (1996).
[32] J. P. Perdew and Y. Wang, Phys. Rev. B **45**, 13244 (1992).
[33] G. Kresse and D. Joubert, Phys. Rev. B **59**, 1758 (1999).
[34] P. E. Blöchl, Phys. Rev. B **50**, 17953 (1994).
[35] G. Kresse, http://cms.mpi.univie.ac.at/vasp-workshop/slides/pseudoppdatabase.pdf
[36] H. J. Monkhorst and J. D. Pack, Phys. Rev. B **13**, 5188 (1976).
[37] M. Methfessel and A. T. Paxton, Phys. Rev. B **40**, 3616 (1989).
[38] P. E. Blöchl, O. Jepsen, and O. K. Andersen, Phys. Rev. B **49**, 16223 (1994).
[39] S. Curtarolo, D. Morgan, and G. Ceder, CALPHAD: Comput. Coupling Phase Diagrams Thermochem. **29**, 163 (2005).
[40] M. H. F. Sluiter, CALPHAD: Comput. Coupling Phase Diagrams Thermochem. **30**, 357 (2006).
[41] M. H. F. Sluiter, Acta Mater. **55**, 3707 (2007).
[42] L. M. Alte da Veiga, Port. Phys. **4**, 205 (1966).

[43] Y. Nishihara, Y. Yamaguchi, M. Tokumoto, K. Takeda, and K. Fukamichi, Phys. Rev. B **34**, 3446 (1986).

[44] R. M. Waterstrat and J. S. Kasper, Trans. Am. Inst. Min., Metall. Pet. Eng. **209**, 872 (1957).

[45] P. Villars, K. Cenzual, J. L. C. Daams, F. Hulliger, T. B. Massalski, H. Okamoto, K. Osaki, A. Prince, and S. Iwata, *Pauling File: Inorganic Materials Database and Design System, Binaries edition* (ASM International, Metal Park, OH, 2003).